**Cell Reports, Volume *32***

## Supplemental Information

# Pseudo-RNA-Binding Domains Mediate RNA Structure Specificity in Upstream of N-Ras

**Nele Merret Hollmann, Pravin Kumar Ankush Jagtap, Pawel Masiewicz, Tanit Guitart, Bernd Simon, Jan Provaznik, Frank Stein, Per Haberkant, Lara Jayne Sweetapple, Laura Villacorta, Dylan Mooijman, Vladimir Benes, Mikhail M. Savitski, Fátima Gebauer, and Janosch Hennig**

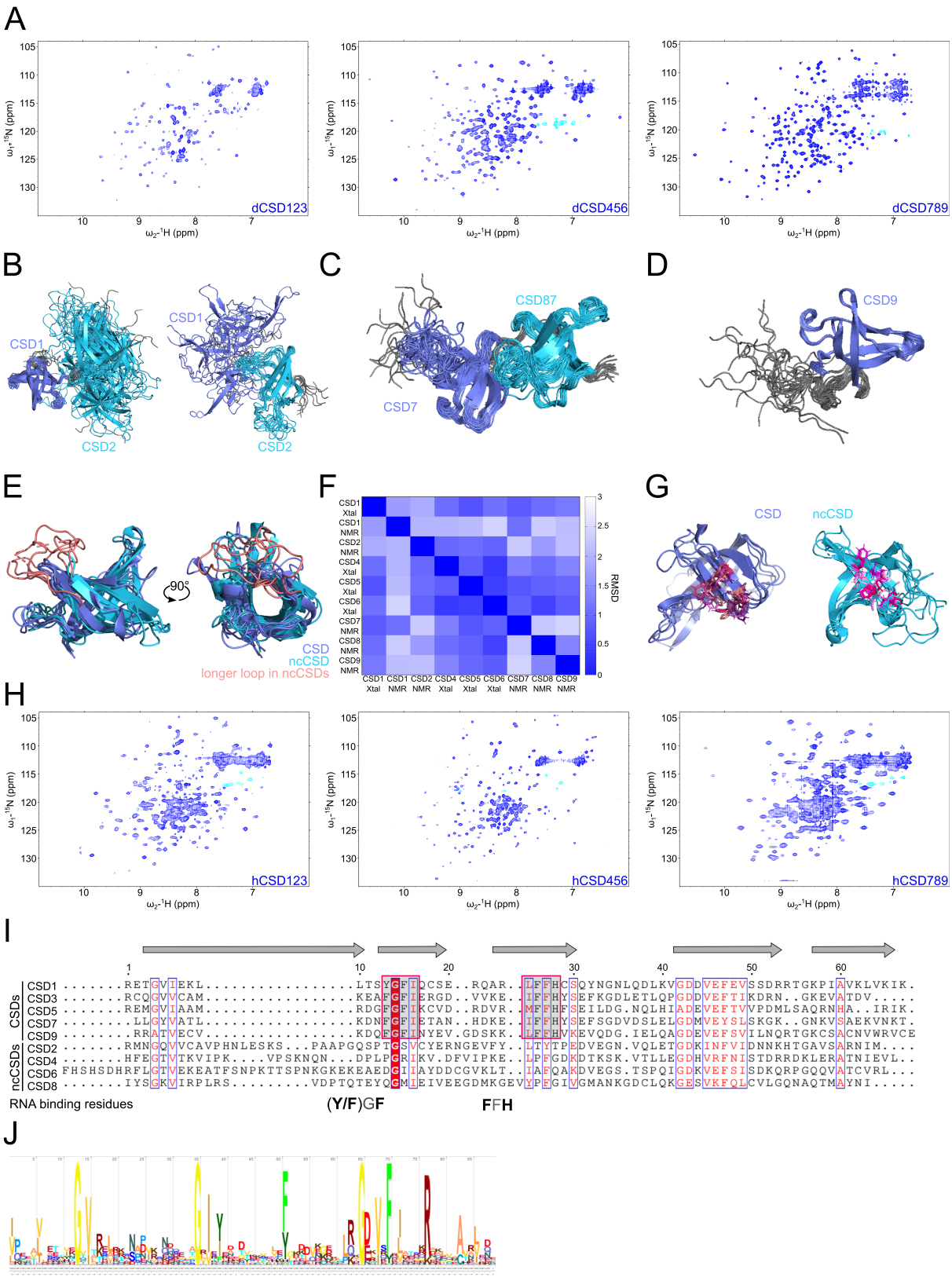


**Supplementary Figure 1, Related to Figure 1:** A: $^{1}$H,$^{15}$N-HSQC spectra of CSD123, CSD456 and CSD789 constructs. B: Ensemble of the 20 lowest energy NMR conformations of CSD12, superimposed on CSD1 (left) (residues: 197-237) and CSD2 (right) (residues: 269-274, 293-296 and 306-328) separately. C: Ensemble of the 20 lowest energy NMR conformations of CSD78 superimposed on secondary structure elements, excluding flexible loops and termini (residues 764-813, 824-834, 843-854, 867-873 and 879-920). D: Ensemble of the 20 lowest energy NMR conformations of CSD9 superimposed on the core CSD domain (residues 912-990). E: Superimposition of canonical CSDs 1, 5,

7 and 9 with ncCSDs 2, 4, 6 and 8. The additional loop that is present only in ncCSDs is highlighted in pink. F: Matrix of RMSD values from superimpositions of each single CSD of dUnr. For the comparison with CSD1 the crystal structure from PDB entry 4QQB was used. G: Superimposition of canonical CSDs 1, 5, 7 and 9 and ncCSDs 2,4,6 and 8 showing the RNA binding residues (F/Y-G-F and F-F-H) or equivalent residues pointing to the outside of the barrel (highlighted in shades of pink). H: $^{1}H,^{15}N$-HSQC spectra of CSD123, CSD456 and CSD789 of human Unr exhibit peak dispersion indicative of folded proteins and similar to dUnr. I: Sequence alignment of canonical and ncCSDs of human Unr. The same or similar residues between all domains are colored, similar residue regions between the canonical CSDs are highlighted by boxes, which align with the two RNA binding regions (Y/FGF and FFH). The alignment has been done using Emboss Needle (Madeira et al., 2019) and ESPript (Robert and Gouet, 2014) has been used for illustration. J: Presentation of the sequence logo that was used for the hidden markov model search.

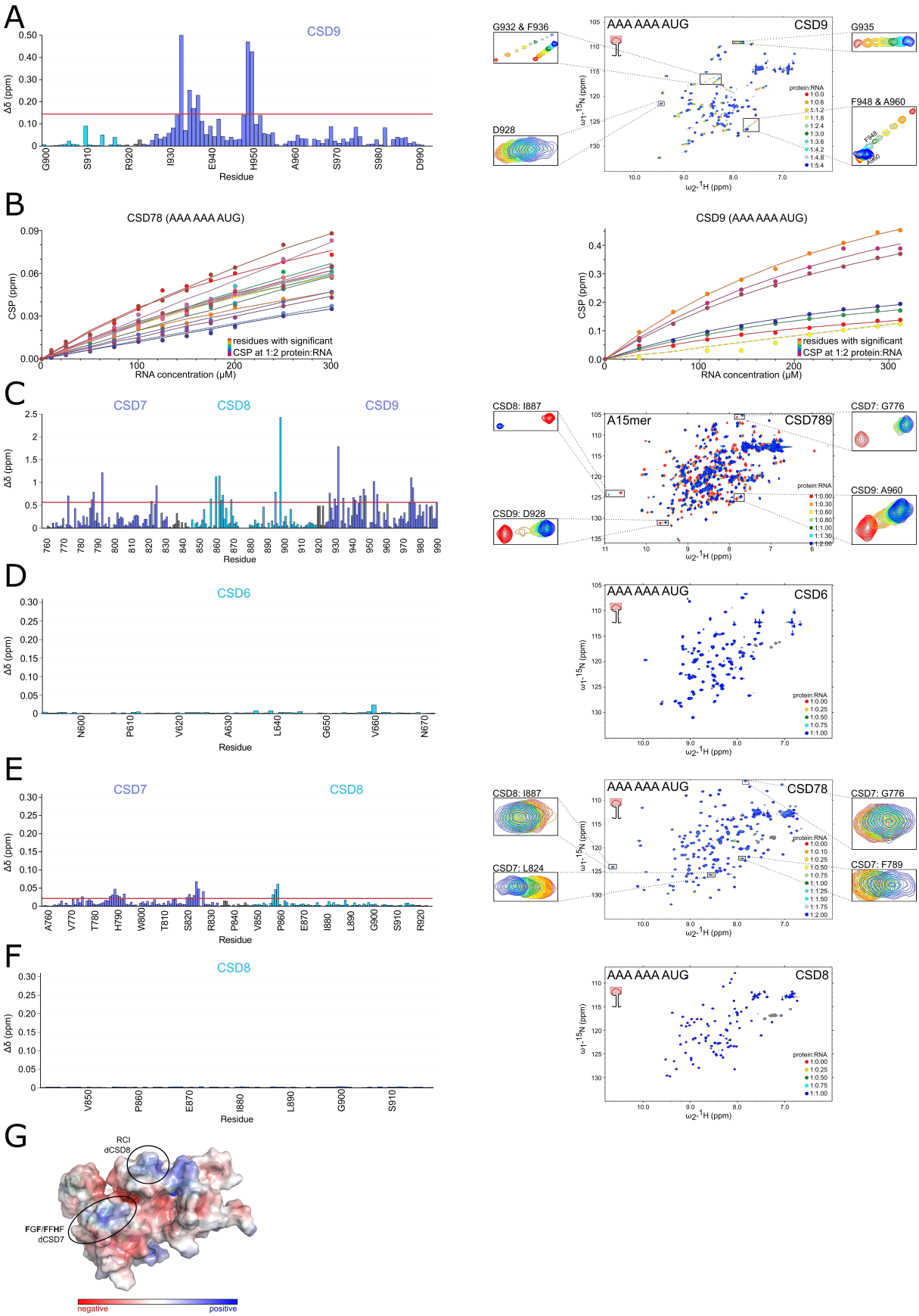


**Supplementary Figure 2, Related to Figure 2:** A: $^{1}$H, $^{15}$N-HSQC NMR titration of CSD9 (898-990) with a 9-mer RNA (AAA AAA AUG) zooming into regions, which show distinct shifts for some residues (right) and a histogram with chemical shift perturbation magnitude at end points per residue (left). B: The chemical shift perturbations and the corresponding fit for the different titration

concentrations for residues shifting significantly (CSP larger than the average plus standard deviation of all shifts) are shown. C: $^{1}H$, $^{15}N$-HSQC NMR titration of CSD789 (756-990) with an A15-mer RNA oligonucleotide zooming into regions, which show exemplary residues with distinct shifts (right) and a histogram with chemical shift perturbation magnitudes at the titration end points per residue (left). D: $^{1}H$, $^{15}N$-HSQC NMR titration of CSD6 (593-677) with a 9-mer RNA (AAA AAA AUG) (right) devoid of significant chemical shift perturbations, as shown also in the CSP plot (left). E: $^{1}H$, $^{15}N$-HSQC NMR titration of CSD78 (756-922) with a 9-mer RNA (AAA AAA AUG) zooming into regions, which show distinct shifts for some residues (right) and a histogram with chemical shift perturbations magnitude at end points per residue (left). F: $^{1}H$, $^{15}N$-HSQC NMR titration of CSD8 (841-922) with a 9-mer RNA (AAA AAA AUG) (right) devoid of significant chemical shift perturbations, as shown also in the CSP plot (left). G: Calculated surface potential for CSD78. Highlighted is the region of RNA binding residues of canonical CSD7 and the region of residues in ncCSD8, that show significant shifts after addition of RNA.

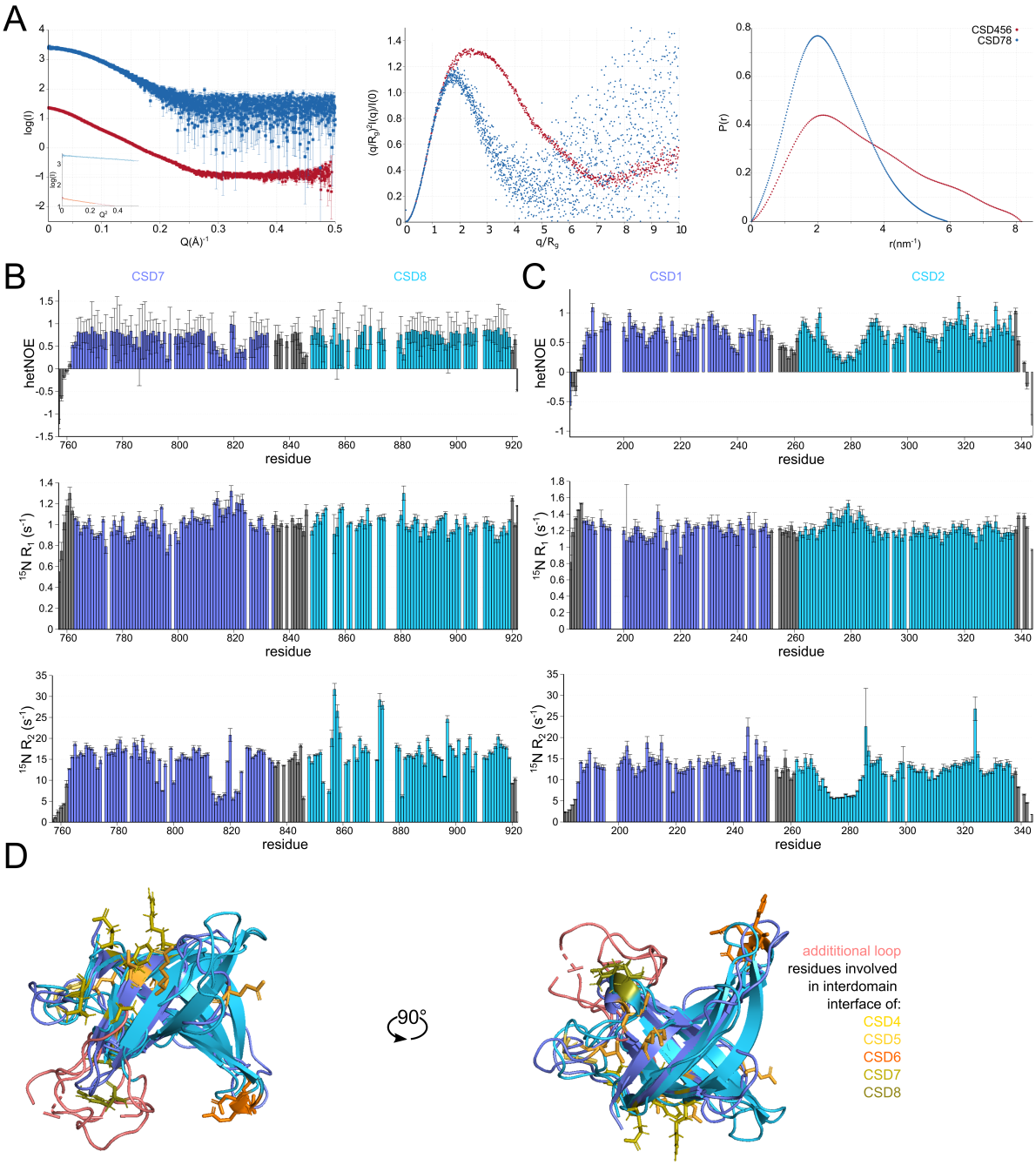


**Supplementary Figure 3, Related to Figure 3:** A left: *I*(*q*) *versus q* as log-linear plots with the inset showing the Guinier fits for $qR_g < 1.3$ indicating good data quality and no aggregation for the curves of CSD456 (red) and CSD78 (blue). Middle: Dimensionless Kratky plots indicate that proteins (CSD456: red; CSD78: blue) are mostly structured with low flexibility. Right: *P*(*r*) *versus r* profiles normalized to equal areas, showing the highest radius of gyration for CSD456 (red) and the lowest for CSD78 (blue). B and C: $^{15}$N relaxation parameters of CSD78 (B) and CSD12 (C) showing the $^{1}$H-$^{15}$N heteronuclear NOEs (hetNOE), the $^{15}$N longitudinal relaxation rates ($^{15}$N $R_1$) and the $^{15}$N transverse relaxation rates ($^{15}$N $R_2$). D: Superimposition of CSD5 and 7 and ncCSD4, 6 and 8, highlighting the additional loop that is present in the ncCSDs (pink) and the residues that are involved in formation of the interdomain interaction surface (shades from yellow to green).

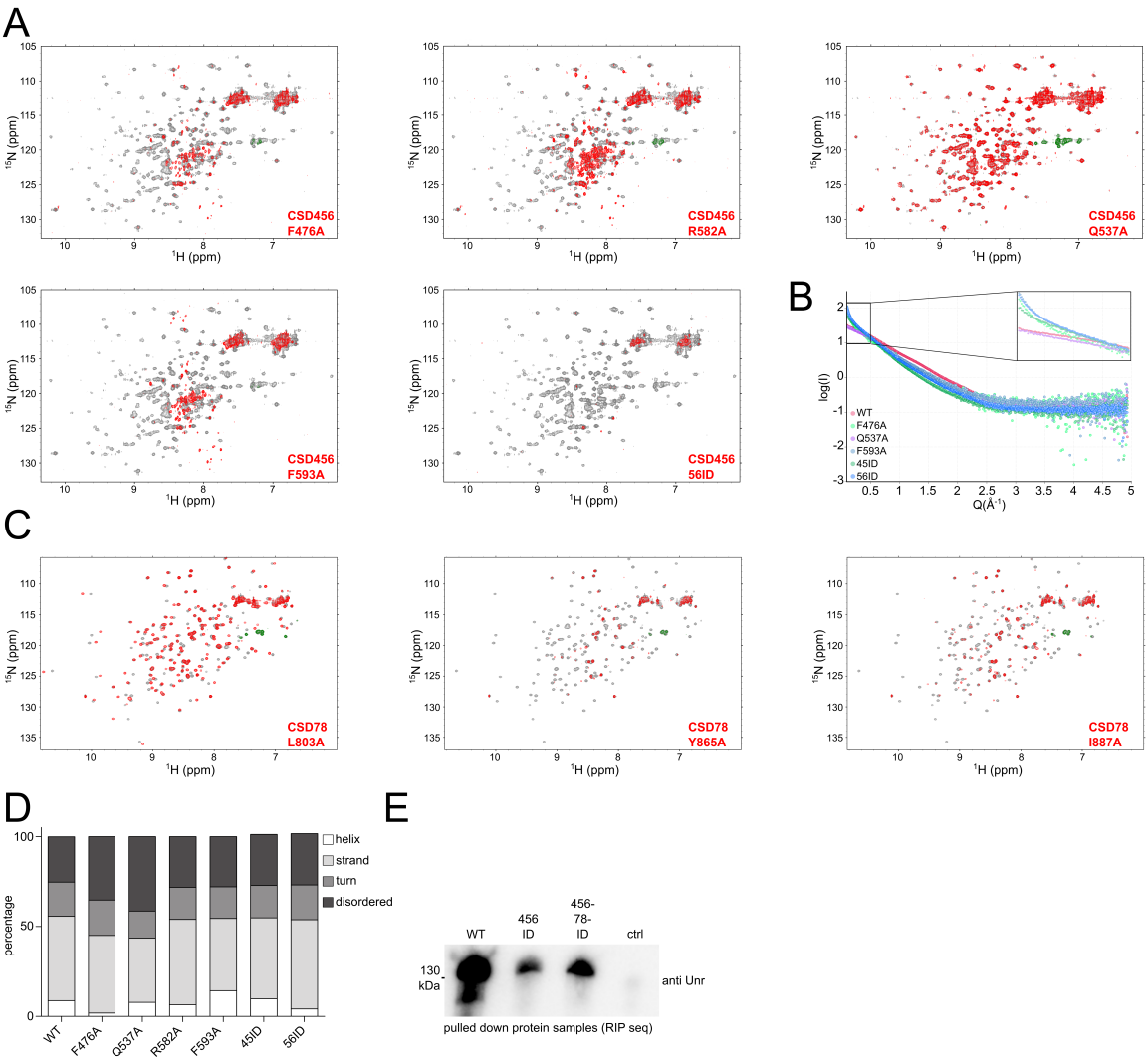


**Supplementary Figure 4, Related to Figure 4**: A: $^{1}H,^{15}N$-HSQC spectra of CSD456 wild type (grey) overlaid with the spectra of CSD456 mutants (red) showing aggregation of most of the mutants compared to the wild type. The proteins had a concentration of 30 µM. B: SAXS curve of CSD456 wild type construct and the different mutants measured at the same concentration (1 mg/ml). Again, except for the Q538A mutant aggregation could be measured. C: $^{1}H,^{15}N$-HSQCs of CSD78 wild type (grey) overlaid with the different spectra of CSD78 mutants (red). The L803A mutant shows CSPs compared to the wild type sample, whereas for the other two mutants aggregation could be observed The proteins had a concentration of 80 µM. D: Prediction of different secondary structure elements (helix, strand, turn and disordered) from CD curves of Unr full-length wt and different interdomain mutants, showing no difference between the wild type and mutant samples. E Western blot showing the efficiency of the Unr pull-down against the V5 tagged wild type and the two interdomain mutants of the samples (456ID, 456-78-ID) used for RIP seq. No protein was detected in the control sample, which was transfected with an empty vector. Unr antibody against an N-terminal part of the protein was used.

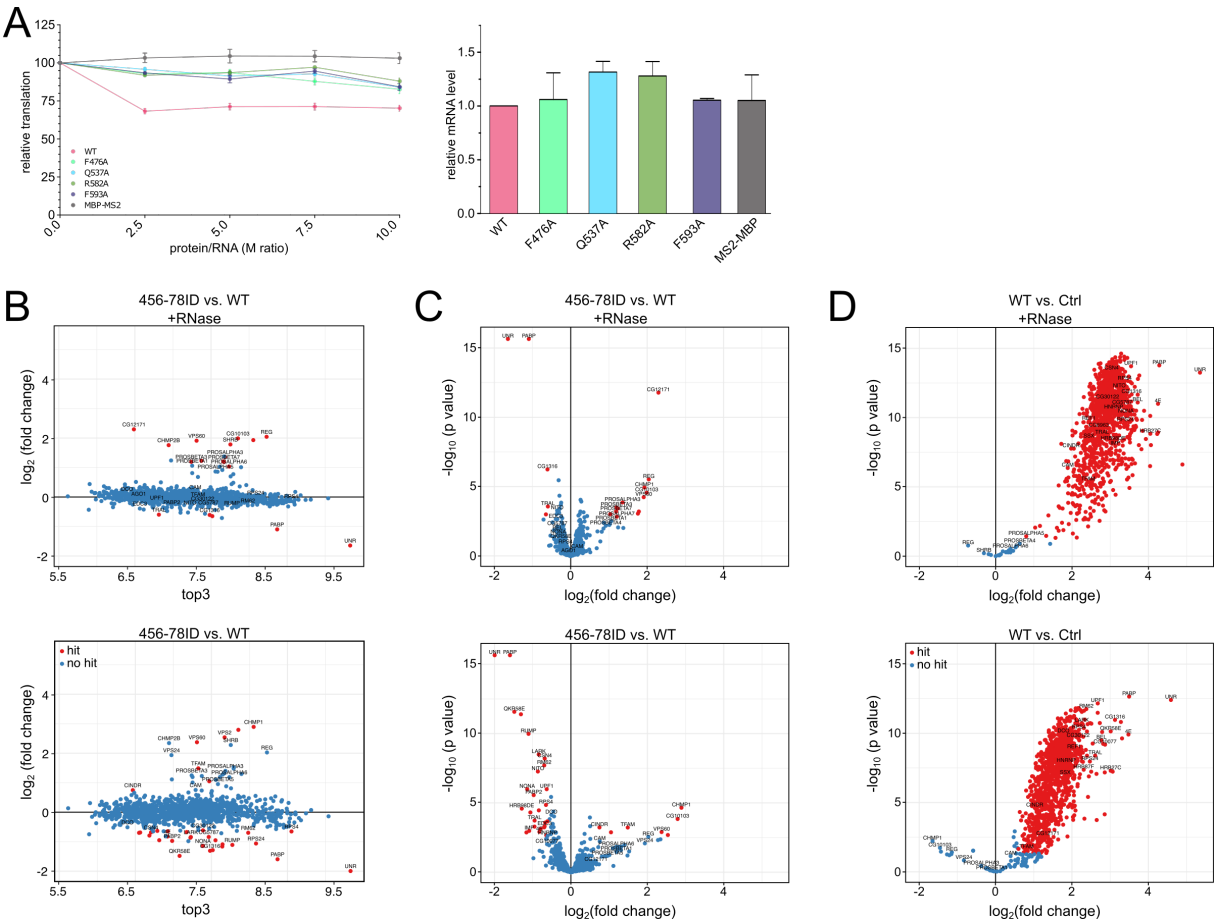


**Supplementary Figure 5, Related to Figure 5**: A left: Relative *in vitro* translation of the Firefly reporter gene over the internal control Renilla after adding different amounts of single dUnr mutants compared to wild type dUnr. N=3. The wild type protein shows a higher translation repression rate than the mutants. The control (MBP-MS2) doesn't show any repression. Right: Relative mRNA levels of the ratio of Renilla and Firefly after in vitro translation experiments, measured by qPCR. N=3 from 2.5 excess of protein over RNA, indicating, that the observed difference in signal is not due to different mRNA levels.. B: Scatter plot showing the top3 value (average abundance of a protein in the mass spectrometry run) versus the log2(fold change) of interdomain mutant vs WT for RNase treated (top) and non-treated (bottom) conditions. N=3. C/D: Volcano plots showing the difference of protein targets of the IP-MS between the WT sample and the 456-78 interdomain mutant (C) or the control (D) with (upper graph) and without RNase treatment (lower graph). The $\log_2$(fold change) is plotted against the negative $\log_{10}$(p value). Differentially regulated proteins are colored in red. D: Due to the low background level of the control sample, almost all proteins were classified as differentially regulated. N=3

**Table S1, Related to Figure 1. List of soluble and unsoluble protein constructs tested for *Drosophila* Unr.**

| boundaries | old nomenclature | new nomenclature | tag |
|---|---|---|---|
| 2-130 | N-temrinus + q-rich | N-temrinus + q-rich | His |
| 2-183 | N-temrinus + q-rich | N-temrinus + q-rich | His |
| 11-130 | N-temrinus + q-rich | N-temrinus + q-rich | His |
| 11-183 | N-temrinus + q-rich | N-temrinus + q-rich | His |
| 176-414 | CSD1/2 | CSD1/2/3 | His |
| 176-669 | CSD123 | CSD1-6 | His |
| 176-677 | CSD123 | CSD1-6 | His |
| 186-252 | CSD1 | CSD1 | His-Trx |
| 186-324 | CSD1 | CSD12 | His |
| 186-339 | CSD1 | CSD12 | His |
| 186-341 | CSD1 | CSD12 | His |
| 186-344 | CSD1 | CSD12 | His |
| 186-414 | CSD1/2 | CSD1/2/3 | His |
| 186-990 | CSD1-5 | CSD1-9 | His |
| 345-515 | CSD2 | CSD34 | His |
| 345-586 | CSD35 | CSD345 | His |
| 422-515 | | CSD4 | His |
| 422-586 | CSD3 | CSD4/5 | His |
| 422-677 | CSD3 | CSD456 | His |
| 422-853 | CSD3/4 | CSD4-7 | His |
| 428-990 | CSD345 | CSD4-9 | His |
| 516-581 | CSD3 | CSD5 | His |
| 516-669 | CSD3 | CSD5/6 | His |
| 593-677 | | CSD6 | His |
| 593-757 | | CSD6 + q-rich | |
| 593-922 | CSD4 | CSD678 | His |
| 678-922 | CSD4 | q-rich + CSD78 | |
| 757--922 | CSD4 | CSD78 | His |
| 757-853 | CSD4 | CSD7 | His |
| 757-856 | CSD4 | CSD7 | His |
| 757-991 | CSD4/5 | CSD7/8/9 | His |
| 856-991 | CSD5 | CSD8/9 | His |
| 899-991 | CSD5 | CSD9 | His |
| 2-52 | N-terminus | N-terminus | His |
| 2-61 | N-terminus | N-terminus | His |
| 11-52 | N-terminus | N-terminus | His |
| 11-61 | N-terminus | N-terminus | His |
| 47-130 | N-temrinus + q-rich | N-temrinus + q-rich | His |
| 47-183 | N-temrinus + q-rich | N-temrinus + q-rich | His |
| 54-130 | q-rich | q-rich | His |

soluble - not used in publication

soluble - used in publication

not soluble

| | | | |
|---|---|---|---|
| 54-183 | q-rich | q-rich | His |
| 62-130 | q-rich | q-rich | His |
| 62-183 | q-rich | q-rich | His |
| 186-1017 | CSD1-5 | CSD1-9 | His |
| 186-669 | CSD123 | CSD1-6 | His |
| 186-677 | CSD123 | CSD1-6 | His |
| 285-424 | CSD2 | CSD2/3 | His |
| 286-502 | CSD2 | CSD34 | His |
| 292-414 | CSD2 | CSD23 | His |
| 293-581 | CSD35 | CSD345 | His |
| 293-586 | CSD35 | CSD345 | His |
| 293-642 | CSD35 | CSD345 | His |
| 293-669 | CSD35 | CSD3456 | His |
| 293-677 | CSD35 | CSD3456 | His |
| 298-502 | CSD2 | CSD34 | His |
| 298-515 | CSD2 | CSD34 | His |
| 345-414 | CSD2 | CSD3 | His |
| 345-414 | CSD2 | CSD3 | His-MBP |
| 345-502 | CSD2 | CSD34 | His |
| 345-581 | CSD35 | CSD345 | His |
| 345-643 | CSD35 | CSD345 | His |
| 345-669 | CSD35 | CSD3456 | His |
| 345-677 | CSD35 | CSD3456 | His |
| 422-1017 | CSD345 | CSD4-9 | His |
| 422-502 | | CSD4 | His |
| 422-581 | CSD3 | CSD4/5 | His |
| 422-642 | CSD3 | CSD45 | His |
| 422-832 | CSD34 | CSD4-7 | His |
| 422-835 | CSD34 | CSD4-7 | His |
| 422-856 | CSD34 | CSD4-7 | His |
| 422-875 | CSD34 | CSD4-7 (8half) | His |
| 422-910 | CSD34 | CSD4-7 (8half) | His |
| 422-910 | CSD34 | CSD4-8 | His |
| 422-990 | CSD345 | CSD4-9 | His |
| 428-1017 | CSD345 | CSD4-9 | His |
| 428-502 | | CSD4 | His |
| 428-515 | | CSD4 | His |
| 428-581 | CSD3 | CSD4/5 | His |
| 428-596 | CSD3 | CSD4/5 | His |
| 446-642 | CSD3 | CSD56 | His |
| 446-832 | CSD34 | CSD4-7 | His |
| 446-835 | CSD34 | CSD4-7 | His |
| 446-853 | CSD34 | CSD4-7 | His |
| 446-856 | CSD34 | CSD4-7 | His |

| | | | |
|---|---|---|---|
| 446-875 | CSD34 | CSD4-7 (8half) | His |
| 446-910 | CSD34 | CSD4-8 | His |
| 516-586 | CSD3 | CSD5 | His |
| 516-586 | CSD3 | CSD5 | His-MBP |
| 516-586 | CSD3 | CSD5 | His |
| 516-677 | CSD3 | CSD5/6 | His |
| 516-832 | CSD34 | CSD5-7 | His |
| 516-835 | CSD34 | CSD5-7 | His |
| 516-853 | CSD34 | CSD5-7 | His |
| 516-856 | CSD34 | CSD5-7 | His |
| 516-875 | CSD34 | CSD5-7 (8half) | His |
| 516-910 | CSD34 | CSD5-8 | His |
| 593-669 | | CSD6 | His |
| 678-757 | q-rich | q-rich | His |
| 678-703 | q-rich | q-rich | His |
| 703-757 | q-rich | q-rich | His |
| 757-1017 | CSD4/5 | CSD7/8/9 | His |
| 757-875 | CSD4 | CSD7 | His |
| 757-890 | CSD4 | CSD78 | His |
| 757-900 | CSD4 | CSD78 | His |
| 757-911 | CSD4 | CSD78 | His |
| 763-832 | CSD4 | CSD7 | His |
| 763-832 | CSD4 | CSD7 | His-MBP |
| 763-910 | CSD4 | CSD7 | His |
| 856-1017 | CSD5 | CSD8/9 | His |
| 899-1017 | CSD5 | CSD9 | His |
| 910-1017 | CSD5 | CSD9 | His |
| 911-990 | CSD5 | CSD9 | His |
| 923-990 | CSD5 | CSD9 | His |
| 345-414 | CSD2 | CSD3 | His-Trx |
| 516-586 | CSD3 | CSD5 | His-Trx |
| 763-832 | CSD4 | CSD7 | His-Trx |
| 923-990 | CSD5 | CSD9 | His-Trx |

**Table S2, Related to Figure 1. Statistics of the NMR structure calculation of *Drosophila* Unr CSD12 bound to SL6 apical RNA, CSD78 and CSD9 and data collection and refinement statistics of the crystal structure of *Drosophila* Unr CSD456.** Statistics for the highest-resolution shell are shown in parentheses.

| **NMR structure statistics** | | | |
|---|---|---|---|
| | **dCSD12+SL6 apical** | **dCSD78** | **dCSD9** |
| | **Experimental restraints** | | |
| Total NOEs | 3911 | 4530 | 3712 |
| distance restraints | 1788 | 2323 | 1831 |
| Short range (\|i − j\| ≤ 1) | 1005 | 1242 | 544 |
| Medium range (\|i − j\| < 5) | 124 | 211 | 283 |
| Long range (\|i − j\| > 5) | 659 | 870 | 1004 |
| Dihedral restraints (ϕ/ψ) | 224 | 167 | 93 |
| | **Structural Quality** | | |
| Coordinate precision (Å) | | | |
| Backbone (N, Cα, C′) | 0.40 (CSD1), 0.53 (CSD2) (a) | 0.39 (CSD7), 0.39 (CSD8) (b) | 0.38 (c) |
| Heavy atoms | 0.99 (CSD1), 1.05 (CSD2) (a) | 0.84 (CSD7), 0.86 (CSD8) (b) | 0.80 (c) |
| Restraint RMSD | | | |
| Distance restraints, Å | 0.02 +/- 0.0019 | 0.0196 +/- 0.002 | 0.0253 +/- 0.003 |
| Dihedral restraints, ° | 0.666 +/- 0.104 | 1.437 +/- 0.101 | 0.565 +/- 0.105 |
| Deviation from idealized geometry | | | |
| Bond lengths, Å | 0.0038 +/- 0.00008 | 0.0036 +/- 0.00009 | 0.00434 +/- 0.00013 |
| Bond angles, ° | 0.504 +/- 0.01 | 0.491 +/- 0.011 | 0.542 +/- 0.022 |
| | **Whatcheck analysis** | | |

| | | | |
|---|---|---|---|
| First generation packing | -3.271 +/- 0.228 | -2.751 +/- 0.161 | -1.912 +/- 0.191 |
| Second-generation packing | -2.491 +/- 0.274 | -2.402 +/- 0.239 | -1.560 +/- 0.284 |
| Ramachandran plot appearance | -3.806 +/- 0.298 | -3.843 +/- 0.329 | -4.442 +/- 0.480 |
| $\chi^{-1}/\chi^{-2}$ rotamer normality | -3.806 +/- 0.532 | -3.915 +/- 0.473 | -5.416 +/- 0.431 |
| Backbone confirmation | -1.261 +/- 0.534 | -2.329 +/- 0.537 | -1.326 +/- 0.376 |
| | **Ramachandran analysis, %** | | |
| Favored regions | 80.9 | 76.7 | 80.5 |
| Allowed regions | 16.7 | 20.9 | 18.9 |
| Generously allowed | 1.9 | 1.7 | 0.6 |
| Disallowed | 0.4 | 0.7 | 0.0 |

| | |
|---|---|
| a | For residues using 197-237 (CSD1) and 269-274, 293-296 and 306-328 (CSD2) |
| b | For residues using 764-813 and 824-834 (CSD7) and 843-854, 867-873 and 879-920 for (CSD8) |
| c | For residues using 912-990 |

| **Crystallography statistics CSD456** | |
|---|---|
| Wavelength | 1.005 Å |
| Resolution range | 77.84 - 2.02 (2.092 - 2.02) |
| Space group | P 62 |
| Unit cell | 89.88 89.88 58.75 90 90 120 |
| Total reflections | 113928 (6419) |
| Unique reflections | 34128 (2534) |
| Multiplicity | 3.3 (2.5) |
| Completeness (%) | 98.00 (87.3) |
| Mean I/sigma(I) | 7.8 (1.0) |
| Wilson B-factor | 39.76 |
| R-merge | 0.073 (0.78) |
| R-meas | 0.087 (0.95) |
| R-pim | 0.046 (0.54) |
| CC1/2 | 0.99 (0.57) |
| Reflections used in refinement | 32428 (2409) |
| Reflections used for R-free | 1698 (124) |

| | |
|---|---|
| R-work | 0.22 (0.32) |
| R-free | 0.25 (0.32) |
| Number of non-hydrogen atoms | 2062 |
| macromolecules | 1842 |
| ligands | 7 |
| solvent | 213 |
| Protein residues | 238 |
| RMS(bonds) | 0.002 |
| RMS(angles) | 0.38 |
| Ramachandran favored (%) | 96.93 |
| Ramachandran allowed (%) | 2.63 |
| Ramachandran outliers (%) | 0.44 |
| Rotamer outliers (%) | 0.00 |
| Average B-factor | 47.73 |
| macromolecules | 47.83 |
| ligands | 51.27 |
| solvent | 46.76 |

**Table S3, Related to Figure 3. Statistics of the SAXS data and processing statistics of *Drosophila* Unr CSD456 and CSD78.**

| | **dCSD456** | **dCSD78** |
|---|---|---|
| (a) Sample Details | | |
| Organism | *E. coli* BL2 (DE3) | *E. coli* BL2 (DE3) |
| Source | *this work* | *this work* |
| Uniprot sequence ID | Q9VSK3 | Q9VSK3 |
| Description | UNR E422-H677, with TEV-cleaved N-terminal His6-tag | UNR A756-K922, with TEV-cleaved N-terminal His6-tag |
| Molecular mass M from chemical composition (Da) | 29.532 | 18.597 |
| loading concentration (mg/ml) | 1.16 and 4.65 mg/ml | 0.8 mg/ml |
| injection volume (ul) | 30 | 30 |
| concentration (uM) | 40/160 | 45 |
| Solvent composition and source | 20 mM Hepes/NaOH pH 7.5, 150 mM NaCl and 1 mM DTT | |
| (b) SAS data collection parameter | | |
| Source and instrument | Grenoble ESRF BM29 with Dectris Pilatus 1M | Hamburg PETRA-III P12 with Dectris Pilatus 6M (REF) |
| Wavelength (A) | 0.9919 | 1.24 |
| Sample-detector distance (m) | 2,867 | 3.0 |
| q-measurement range (nm-1) | 0.0355-4.9391 | 0.0224-7.3176 |
| Radiation daage monitoring | frame-by-frame comparison | |
| Exposure time (s) & number | 1.0x10 | 0.195x20 |
| Sample configuration | sample chamger with flow through capillary measurement | |
| Sample temperature (°C) | 20 | 25 |
| (c) Software employed for SAS data reduction, analysis and interprtation | | |
| SAXS data processing | I(q) vs. q using Bsx cube, solvent subtraction and curve merging using PRIMUSqt from ATSAS (Franke et al., 2017) | |
| Basic analyses: Guinier, P(r), Vp | PRIMUSqt from ATSAS 2.7.1 (Franke et al., 2017) | |

| | | |
|---|---|---|
| Atomic structure modelling | CRYSOL 2.8.2 from PRIMUSqt in ATSAS 2.8 (Svergun et al., 1995) | |
| Molecular graphics | -- | -- |
| (d) Structural parameters | | |
| | Guinier analysis | |
| I(0) (raw) | 22.8+/-0.06 | 25.4+/-0.05 |
| $R_g$ (Å) | 26.7+/-0.1 | 18.1+/-0.01 |
| $qR_g$ max ($q_{min}$ = 0.0066 Å$^{-1}$) | 1.28 | 1.3 |
| Coefficient of correlation, $R^2$ | 0.97 | 0.74 |
| | P(r) Analysis from AUTOGNOM | |
| I(0) (cm-1) | 22.8 | 25.43 |
| $R_g$ (Å) | 22.61 | 18.2 |
| $d_{max}$ (Å) | 81.5 | 59.1 |
| $q$ range (Å$^{-1}$) | 0.102-3.00 | 0.089-4.427 |
| $\chi^2$ (total estimate from *GNOM*) | 0.67 | 0.89 |
| Porod volume (Å$^{-3}$) (ratio $V_P$/calculated *M)* | 37490 | 27610 |
| (f) Atomistic modelling | | |
| Method | CRYSOL (Svergun et al., 1995) | |
| Crystal stucture | UNR CSD456 (6Y6E) | UNR CSD78 (6Y4H) |
| CRYSOL | Constant subtraction allowed | |
| $\chi^2$ | 1,026 | 1,218 |
| Predicted $R_g$ (Å) | 26.22 | 18.09 |
| Vol (Å), Ra (Å), Dro (e Å$^{-3}$) | 25504, 1.4, 0.07 | 17716, 1.8, 0.000 |

**Table S5, Related to STAR Methods. Sequences for DNA oligonucleotides.**

| REAGENT or RESOURCE | SOURCE | IDENTIFIER |
|---|---|---|
| RNAi targeting Unr forward primer: TAATACGACTCACTATAGGGATTGCTGAAGAAGTTGTATAAGCAA | Militti et al., 2014 | N/A |
| RNAi targeting Unr reverse primer: TAATACGACTCACTATAGGGACACTTGGATTTCAATTTCGTTTTGC | Militti et al., 2014 | N/A |
| RNAi targeting GFP forward primer: TAATACGACTCACTATAGGGCCTGAAGTTCATCTGCACCA | Militti et al., 2014 | N/A |
| RNAi targeting GFP reverse primer: TAATACGACTCACTATAGGGTGAAATTTGTGATGCTATTGCTTT | Militti et al., 2014 | N/A |
| forward qPCR primer against firefly luciferase used in *in vitro* translation assay: TTGTTTCCAAAAAGGGGTTG | Graindorge et al., 2013 | N/A |
| reverse qPCR primer against firefly luciferase used in *in vitro* translation assay: CATCGACTGAAATCCCTGGT | Graindorge et al., 2013 | N/A |
| forward qPCR primer against renilla luciferase used in *in vitro* translation assay: TATTGCTTTGATCTTATCTTGATGC | This paper | N/A |
| reverse qPCR primer against renilla luciferase used in *in vitro* translation assay: ACAAATATCTTACTGCATGGTTTG | This paper | N/A |
| forward qPCR primer against β-galactosidase used in cell assay: AACGTCGTGACTGGGAAAAC | Graindorge et al., 2013 | N/A |
| reverse qPCR primer against β-galactosidase used in cell assay: GGCCTCTTCGCTATTACGC | Graindorge et al., 2013 | N/A |
| forward qPCR primer against renilla luciferase used in cell assay: ACAAGTACCTCACCGCTTGG | Graindorge et al., 2013 | N/A |
| reverse qPCR primer renilla luciferase used in cell assay: GACACTCTCAGCATGGACGA | Graindorge et al., 2013 | N/A |